Supplementary Material

Versatile coordination polymer catalyst for acid reactions involving biobased heterocyclic chemicals

Margarida M. Antunes, Ricardo F. Mendes, Filipe A. Almeida Paz and Anabela A. Valente*

Department of Chemistry, CICECO—Aveiro Institute of Materials, University of Aveiro, 3810-193, Aveiro, Portugal

1. Experimental – Synthesis of the MOF catalyst $[Gd(H_4nmp)(H_2O)_2]Cl{\cdot}2H_2O$ (1)

The synthesis of material **1** was scaled-up from the experimental conditions reported previously [1]. A reactive mixture composed of 0.4635 g (1.554 mmol) of nitrilotris(methylenephosphonic acid) [H_6nmp, $N(CH_2PO_3H_2)_3$, 97 %, Fluka] and 0.4899 g (1.485 mmol) of gadolinium(III) oxide (Gd_2O_3 at least 99.99 %, Jinan Henghua Sci. & Tec. Co. Ltd) in *ca.* 9 mL of distilled water and 9 mL of hydrochloric acid 6M was prepared at ambient temperature inside a 35 mL IntelliVent microwave reactor. Reaction took place inside a CEM Focused Microwave Synthesis System Discover S-Class equipment, under constant magnetic stirring (controlled by the microwave equipment) using an irradiation power of 75 W at 70 °C for 40 min. A constant flow of air (*ca.* 20-30 psi of pressure) ensured a close control of the temperature inside the reactor. The resulting product, $[Gd(H_4nmp)(H_2O)_2]Cl{\cdot}2H_2O$ (**1**), was isolated as a white microcrystalline powder and it was recovered by vacuum filtration, washed with copious amounts of distilled water and then air-dried at ambient temperature.

2. Additional Characterization

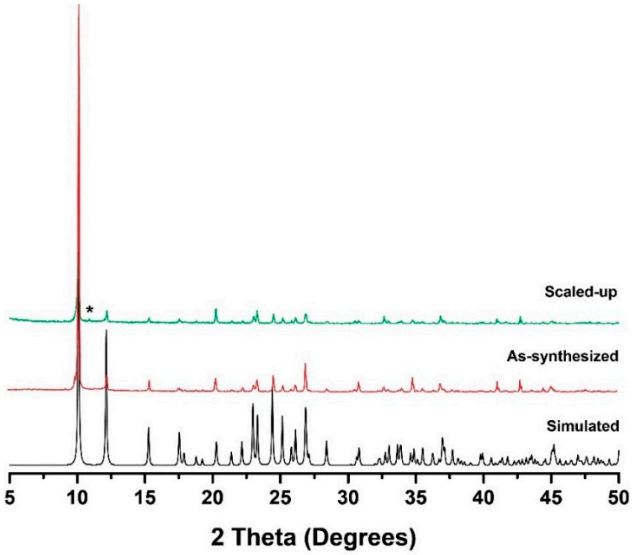

Figure S1: Powder X-ray diffraction of $[Gd(H_4nmp)(H_2O)_2]Cl{\cdot}2H_2O$ (**1**) simulated (black), synthesized using the previously reported synthetic approach (red) and obtained using the scale-up synthesis in this work.

In the PXRD pattern of **1** in Figure S2, a small impurity is represented by an asterisk (*), which was inactive, by comparison of the catalytic results for Fur/Gly reaction in the presence of **1** prepared in the present work, and those for Fur/Gly reaction in the presence of a pure sample of the same MOF prepared in very small scale (synthesis protocol reported previously by us [1]). For the two samples, the catalytic results at 4 h/50 °C were similar, within the range of experimental error.

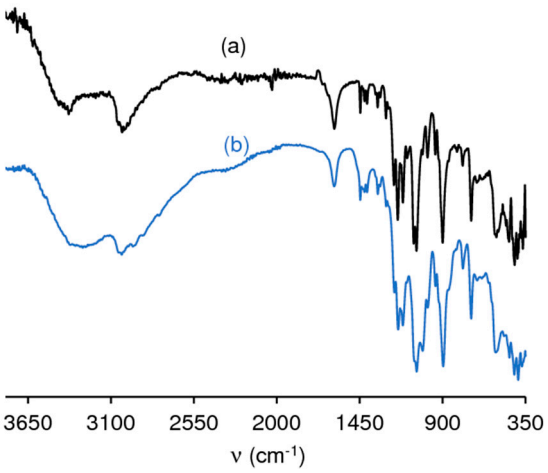

Figure S2: ATR FT-IR spectra of the fresh (a) and used (b) catalyst (Fur/Gly reaction at 50 °C).

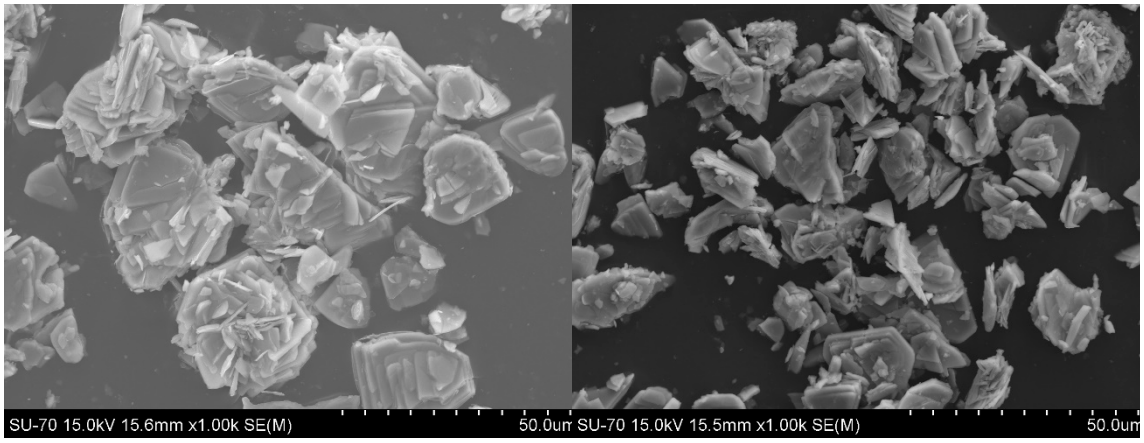

Figure S3: SEM images of [Gd(H$_4$nmp)(H$_2$O)$_2$]Cl·2H$_2$O (**1**) before (a) and after (b) the catalytic reaction of Fur/Gly at 90 °C.

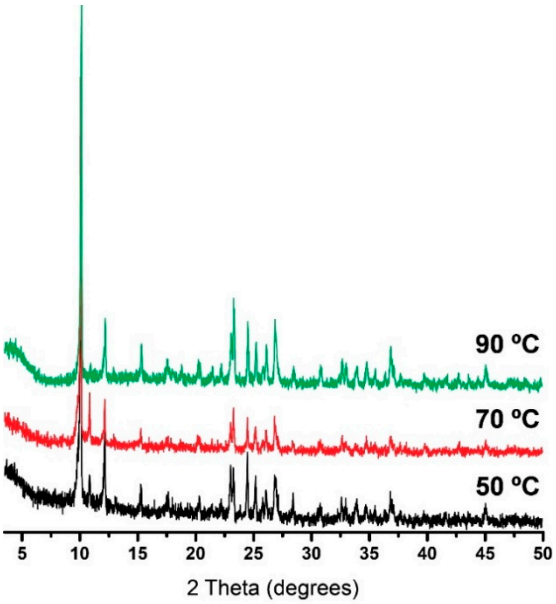

Figure S4: Powder X-ray diffraction of [Gd(H_4nmp)(H_2O)$_2$]Cl·2H_2O (**1**) after the catalytic reaction of Fur/Gly at different reaction temperatures.

3. Comparison of the catalytic results for 1 to literature data for other types of catalysts teste for the FA/ethanol reaction

To the best of our knowledge, there are only two MOFs reported in the literature for the FA conversion to EMF/EL: Hf-UiO-66-SO_3H [2] and MIL-101 (Cr)-SO_3H [3, 4], which are discussed in the main text. In this section, a comparison to other types of catalysts is made (Table S1).
The organocatalyst HCC-ML-SO^3H led to a high EL yield of 85 % at 90 °C/8 h, albeit using a mass ratio of catalyst/substrate which was three times greater than that used for **1** (58 % EL yield at 90 °C/24 h) [5]. A zirconium phosphate catalyst treated with sulfuric acid (ZPS-0.5) led to 93 % EL yield at 140 °C/3 h [6]. MOF **1** led to a similar EL yield to a sulphated attalpugite (H_2SO_4/ATTP) (45-49 % EL yield, at 140 °C), albeit **1** led to approximately the same EL yield in 1 h (instead of 2 h for H_2SO_4/ATTP) and using one third of catalyst/FA mass ratio, as well as *ca.* 4 times more FA concentration [7]. The sulphated nano TiO_2 [8] led to 50 % EL at 130 °C/2 h using 4 times less FA concentration (0.08 vs 0.33 M for **1**) and 10 times less catalyst/FA mass ratio than **1** [8], while the sulphated oxide SO_4^{2-}/TiO_2 [9] led to 68 % EL in 2.5 h, but at 200 °C [9] (Table S1). The results for **1** (63 % EL yield at 140 °C/ 3 h) compared favourably to a SO_4^{-2}/Al_2O_3 catalyst [10] which led to a lower 58 % EL yield at 160 °C/3 h; moreover, for **1** double the concentration of FA (0.33 versus 0.15 M for SO_4^{-2}/Al_2O_3) and 1.6 less catalyst/FA mass ratio were used. MOF **1** also compared favourably to: (a) zeolite H-Beta [11] which was quite active (100 % FA conversion at 110 °C/1.5 h), but led to low selectivity towards the desired products (23 % EL and 14 % EMF versus 25 % EL and 37% EMF at 67 % FA conversion, 90 °C /5 h for **1**); (b) mesoporous aluminosilicate SBA-15 [12] which led to 34 % of EL selectivity at 110 °C/ 6 h (100 % FA conversion; EMF formation was not mentioned); (c) cross-linked ionic liquid polymer PDVB [13] which led to 48 % EL yield at 130 °C/18 h; (d) Zr-Al-mp [14] and mesoporous aluminosilicate Al-TUD-1(21) [15] which give 80 % EL yield at 140 °C/ 24 h, and Al-TUD-1 (4) (51 % EL yield at 140 °C/24 h) [16]; (e) carbon silica composite (CST-1) [17] which led to a similar EL yield at 140 °C/ 6 h (78 %) to **1** at 140 °C/ 5 h (76 %), albeit for CST-1 the EL yield did not increase with reaction time until 24 h (80 % EL) whereas **1** led to 92 % EL yield.

Nanomaterial SAPO-34 [18], sulfonated functional carbon material S-FCM [19] and carbon nanomaterial S-O-NCM [20] led to 69-75 % EL yield at 6-7 h and 130-160 °C, comparable to that for **1** used in a lower catalyst/FA mass ratio (72 % at 140 °C/5 h). Similar results to **1** were reported by some of us for a niobium oxide nanomaterial (Nb_2O_5-NP) (72-73 % EL yield at 140 °C/ 3 h) [21] and GO [22], which led to 63 % EL at 130 °C/2 h) used in a lower catalyst/FA mass ratio (0.01 versus 0.30 for **1**). Other authors used GO in a similar catalyst/FA mass ratio as for **1** (0.25) which led to a higher EL yield of 96 % at 120 °C/6 h (comparable to that for **1** at 140 °C/24 h) [23]. MOF **1** led to comparable results to resin Amberlyst-15 [24] (77 % EL yield at 4 h versus 72 % EL yield at 5 h for **1**) albeit at higher temperature (110 °C for the resin and 140 °C for **1**). Composite C/SBA-15(45) led to 78 % EL yield at 110 °C/24 h, which is somewhat intermediate of that reached for **1** at 90 °C/24 h (58 %) and 140 °C/24 h (92 %) [25]. A silica supported perchloric acid [26] surpassed **1**, since it led to a higher EL yield (84 % yield versus 72 % at 5 h for **1**) at a lower temperature (120 °C versus 140 °C for **1**), using a lower catalyst/FA mass ratio (0.04 versus 0.30) and a higher FA initial concentration (0.51 versus 0.33 M). Superior results were also verified for HPW-MesoZSM-5 [27], Ti-HPA [28], Fe-USY [29] and magnetic sulphated zirconia (MSZ) [30] which led to 91- 97 % EL yield at 120-130 °C and 0.5 - 5 h (for **1**: 72 % EL at 140 °C/ 5 h); a higher FA initial concentration was used for HPW-MesoZSM-5 and MSZ (1.04 - 3.12 M versus 0.33 M for **1**) [27], and a lower catalyst/FA mass ratio was used for HPW-MesoZSM-5 [27], Ti-HPA [28], Fe-USY [29] and MSZ (0.02-0.07 versus 0.33 for **1**) [30]. However, MSZ requires catalyst regeneration at 500 °C to keep the catalytic performance steady, whereas **1** does not require thermal regeneration.

SO_4^{2-}/ZrO_2 [31] and organosilica nanotubes functionalized with arene sulfonic acid and phenyl groups ($ArSO_3HSi(Et)Si$-Ph-NTs [32] and an arylsulfonic acid functionalized hollow mesoporous carbon spheres ($ArSO_3H$-HMCSs.3.2.1 [33]) led to 86-96 % EL yield at (2 h-3 h)/(120 - 140 °C), which was similar to **1** at 24 h/140 °C, albeit the former was used in a much lower amount of catalyst (0.01-0.02 catalyst/FA mass ratio versus 0.3 for **1**) [31]. Organosilica nanotube $12.1PW_{12}/ZrO_2$-Si(Et)Si-NTs1.0 [34] at 120 °C/3 h led to similar results (70 % EL yield) to **1** at 3 h/ 140 °C (72 % EL yield). On the other hand, a sulfonic acid functionalized organosilica nanohybrid ($Si(Et)Si-ArSO_3H$-NHS7.6 [35]) at 120 °C/2 h (60 % EL yield) led to similar results to **1** at 90 °C/24 h (58 % EL yield). Niobium pentoxide nanowires (wNb_2O_5) [36] and Zr-SBA-15(0.09) [37] led to 100 % FA conversion at 140 °C/5 h and 78 %/5 h, respectively, albeit low EL yields (2-9 %) being a more favourable catalyst for targeting EMF (80-87 % yield). An activated carbon led to 75 % EL yield at 170 °C/5 min (comparable to **1** at 140 °C/5 h), although the conditions used in that work were very different: microwave irradiation versus conventional conductive heating for **1**; catalyst/FA mass ratio = 1.70 versus 0.30 for **1**; and FA initial concentration of 0.2 M versus 0.33 M for **1** [38]. A glucose carbonaceous carbon catalyst led to 67 % EL at 150 °C/1 h (**1** led to 37 % at 140 °C/1 h); however, for that catalyst the EL yield decreased with time, whereas for **1** 92 % EL yield was reached within 24 h [39]. Nano ZSM-5 led to 91 % at 140 °C/1 h [22]; **1** required 24 h to reach a similar EL yield of 92 %, using a similar FA concentration (0.33-0.39 M), but requiring a much lower catalyst/FA mass ratio (0.30 for **1** versus 1.02 for ZSM-5). Commercial ZSM-5(50) led to poorer catalytic results to **1** even at 170 °C (59 % EL yield) [40], whereas ZSM-5(25) [41] and hierarchical ZSM-5(30) [42] led to comparable results (53 % EL yield at 70 °C/18 h and 20 % EL at 100 °C/ 2 h, respectively, versus 58 % EL at 90 °C/24 h for **1**).

Overall, the catalytic performance of **1** stands on an intermediate footing among the various types of solid acid catalysts reported in the literature for the FA/ethanol system.

Table S1: Comparison of the catalytic results for **1** to literature data for other acid catalysts studied in the FA/ethanol reaction system[a] [2-49].

Catalyst (solvent)	T (°C)	$[FA]_0$ (M)	Cat:FA (wt)	t (h)	FA conv. (%)	EMF yield (%)	EL yield (%)	Total yield (%)	Ref.
1	90	0.33	0.30	1/5/24	8/67/100	2/52/35	0/25/58	2/62/93	-
1	140	0.33	0.30	1/5/24	90/100/100	37/18/3	49/72/92	86/90/95	-
UiO-66(Hf)-SO_3H	120	0.05	~1.26	4	nm	nm	62	nm	[2]
MIL-101 (Cr), MMS(0.3)-0.15	140	0.28	0.44	2	100	3	76	79	[3]
MIL-101-Cr-SO_3H	140	0.28	1.02	2	100	0	79	79	[4]
HCC-ML-SO_3H	90	0.20	1.02	8	100	nm	85	nm-	[5]
Zr-PS-0.5	140	0.33	0.25	3	100	1	93	94	[6]
PDVB-IL polymer	130	0.58	1.5	12	100	nm	48	nm	[13]
Glucose-carbonaceous carbon	150	0.41	0.5	1	nm	nm	67	nm	[39]
Sulfated attalpugite (H_2SO_4/ATTP)	140	0.08	1	2	90	nm	45	.	[7]
Sulfated TiO_2 nanosheeets	130	0.08	0.03	2	100	nm	51	-	[8]
SO_4^{2-}/TiO_2	200	0.58	0.44	2.5	nm	nm	68	nm	[9]
Magnetic sulfated zirconia (SZF)	120	1.04	0.07	2	100	-	96	-	[30]
SO_4^{2-}/Al_2O_3	160	0.15	0.5	3	100	nm	58	-	[10]
SO_4^{2-}/ZrO_2	130	0.08	0.01	2	100	-	96	.	[31]
Nano-Carbon (S-O-NCM)	130	nm	0.25	7	95	20	75	95	[20]
S-R-NCM	130	nm	0.25	7	98	44	52	96	[20]
NS-FCM	150	0.17	0.5	5	78	-	62	-	[19]
S-FCM	150	0.17	0.5	6	100	-	69	-	[19]
Activated carbon, mW	170	0.2	1.70	0.08	100	nm	75	-	[38]
GO	130	0.51	0.01	2	100	-	63	-	[22]
GO	120	0.33	0.25	6	100	<1	96	96	[23]
C-SBA-15(45)	110	0.33	0.30	24	100	2	77	79	[25]
CST-1	140	0.33	0.30	6/24	100	0	78/80	78/80	[17]
Amberlyst-15	110	0.3	0.17	4	100	6	77	83	[24]
Amberlyst-15 (10 wt% H_2O)	45	0.08	2.2	0.17	nm	nm	67	67	[43]
H-ClO_4-SiO_2	120	0.51	0.04	6	nm	nm	84	nm	[26]
wNb_2O_5	140	1.05	0.22	5	100	80	9	92	[36]
Nb_2O_5-NP	140	0.33	0.21	3	100	23	73	96	[21]
-Fe_2O_3	250	0.02	35.4	1	100	nm	73	nm	[44]
$H_1Cs_2PW_{12}O_{40}$	110	1.05	0.05	2.5	58	32	3	36	[45]
Al_2O_3/SiO_2 [b, c]	180	1.03	nm	- [c]	100	-	90	-	[46]
Ti-TPA	120	0.24	0.02	0.5	100	5	95	100	[28]
ZrAl-mp	140	0.33	0.30	24	100	4	80	84	[14]
NanoSAPO-34	160	0.24	0.53	6	100	1	74	81	[18]
Mesoporous ZSM-5	140	0.39	1.02	1	100	-	90	-	[47]
Hierarchical ZSM-5(30)	100	1.8	0.1	2	nm	12	20	32	[42]
ZSM-5(30)	40	1.04	0.2	2	9	7	-	7	[48]
ZSM-5(30) [b]	125	0.60	nm	nm	100	-	65	65	[49]
HZSM-5(25)	70	0.94	0.8	18	98	24	53	77	[41]
ZSM-5(50) [b]	170	1.6	0.09	nm	100	1	59	60	[40]
SBA-15	110	0.15	4.1	6	95	nm	34	-	[12]
ZrSBA-15	78	0.57	0.34	5	95	87	2	89	[37]
Al-TUD-1(21)	140	0.33	0.3	24	100	-	80	80	[15]
Al-TUD-1(4)	140	0.33	0.3	24	100	4	51	55	[16]
HPW-ZSM-5	120	3.12	0.25	5	100	3	97	100	[27]

USY	120	0.20	0.02	4	91	-	67	-	[29]
Fe-USY	120	0.20	0.02	4	85	-	74	-	[29]
Fe-USY	130	0.20	0.03	4	99	-	91	-	[29]
H-Beta	110	0.28	0.4	1.5	100	15	23	38	[11]
$ArSO_3HSi(Et)Si$-Ph-NTs)	120	0.28	0.02	2	100	nm	85	nm	[32]
$ArSO_3H$-HMCSs3.2.1	140	0.28	0.02	2	nm	nm	86	nm	[33]
$Si(Et)Si$-$ArSO_3H$-HNS7.6	120	0.28	0.02	2	nm	nm	60	nm	[35]
$12.1PW_{12}/ZrO_2$-Si(Et)Si-NTs1.0	120	0.28	0.05	3	100	nm	70	nm	[34]

[a] nm = not mentioned, the reaction conditions are specified, namely the reaction temperature (T), initial furfuryl alcohol concentration ([FA]0 (M)), catalyst/FA mass ratio and time (t). HCC-ML-SO_3H = microporous sulphonated monolithic catalyst, Zr-PS-0.5 = zirconium phosphate with sulfuric acid, PDVB-IL polymer = cross linked polymer of divinylbenzene with acid ionic liquid, NS-FCM and S-FCM = carbon materials possessing amino and sulfonate groups, CST-1 = carbon silica composite; Nb_2O_5-NP = niobium pentoxide nanomaterials, Ti-TPA = titanium exchanged heteropoly tungstophosphoric acid, ZrAl-mp = zirconium–tungsten–aluminium mixed oxides, HPW-ZSM-5 = heteropolyacid supported on mesoporous ZSM-5, $ArSO_3HSi(Et)Si$-Ph-NTs = ethane-bridged organosilica nanotubes functionalized with arene sulfonic acid and phenyl groups, $ArSO_3H$-HMCSs3.2.1 = arylsulfonic acid functionalized hollow mesoporous carbon spheres, $Si(Et)Si$-$ArSO_3H$-HNS7.6 = organosilica nanohybrid, $12.1PW_{12}/ZrO_2$-Si(Et)Si-NTs1.0 = heteropoly acid and ZrO_2 bifunctionalized organosilica nanotubes. [b] Studied in continuous operation mode; [c] 1 h time on stream.

References

[1] Mirante, F.; Mendes, R. M.; Paz, F.A.A.; Balula, S. S. *Catalysts* **2020**, *10*, 731.
[2] Gupta, S.S.R. ; Kantam, M. L. *Catal. Commun*. **2019**, *124*, 62-66.
[3] Liu, X. ; Pan, H. ; Zhang, H.; Li, H. ; Yang, S. *ACS Omega* **2019**, *4*, 8390-8399.
[4] Liu, X.-F.; Li, H.; Zhang, H.; Pan, H.; Huang, S.; Yang, K.-L.; Yang, S. *RSC Adv*. **2016**, *6*, 90232-90238.
[5] Islam, M. M.; Bhunia,S.; Molla, R. A.; Bhaumik, A.; Islam, S. M. *ChemistrySelect* **2016**, *1*, 6079-6085.
[6] Zhai, P.; Lv, G.; Cai, Z.; Zhu, Y.; Li, H.; Zhang, X.; Wang, F. *ChemistrySelect* **2019**, *4*, 3940-3947.
[7] Tian, H.; Shao, Y.; Liang, C.; Xu, Q.; Zhang, L.; Zhang, S.; Liu, S.; Hu, X. *Renew. Energ.* **2020**, *162*, 1576-1586.
[8] Shao, Y.; Du, W.; Gao, Z.; Sun, K.; Zhang, Z.; Li, Q.; Zhang, L.; Zhang, S.; Liu, Q.; Hu, X. *J. Chem. Technol. Biot.* **2020**, *95*, 1337-1347.
[9] Zhao, G.; Hu, L.; Sun, Y.; Zeng, X.; Lin, L. *BioResources* **2014**, *9*, 2634-2644.
[10] Zhang, Z.; Yuan, H.; Wang, Y.; Ke, Y. J. *Solid State Chem*. **2019**, *280*, 120991.
[11] Paniagua, M.; Melero, J. A.; Iglesias, J.; Morales, G.; Hernández, B.; López-Aguado, C. *Appl. Catal. A: Gen.* **2017**, *537*, 74-82.
[12] Enumula, S. S.; Koppadi, K. S.; Gurram, V. R. B.; Burri, D.R. ; Kamaraju, S. R. R. Sustain. *Energy Fuels* **2017**, *1*, 644-651.
[13] Zhou, H.; Song, J.; Kang, X.; Hu, J.; Yang, Y.; Fan, H.; Meng, Q.; Han, B. *RSC Adv.* **2015**, *5*, 15267-15273.
[14] Neves, P.; Russo, P.A.; Fernandes, A.; Antunes, M. M.; Farinha, J.; Pillinger, M.; Ribeiro, M. F.; Castanheiro, J. E.; Valente, A. A. *Appl. Catal. A: Gen*. **2014**, *487*, 148-157.
[15] Neves, P.; Lima, S.; Pillinger,M.; Rocha, S. M.; Rocha, J.; Valente, A. A., *Catal. Today* **2013**, *218-219*, 76-84.
[16] Neves, P.; Antunes, M. M.; Russo, P.A.; Abrantes, J. P.; Lima, S.; Fernandes, A.; Pillinger, M.; Rocha, S. M.; Ribeiro, M. F.; Valente, A. A. *Green Chem*. **2013**, *15*, 3367-3376.
[17] P Russo, P. A.; Antunes, M. M.; Neves, P., Wiper, V. P.; Fazio, E.; Neri, F.; Barreca, F.; Mafra, L.; Pillinger, M.; Pinna, N.; Valente, A. A. *J. Mater. Chem. A* **2014**, *2*, 11813-11824.
[18] Guo, Q.; Yang, F.; Liu, X.; Sun, M.; Guo, Y.; Wang, Y. *Chinese J. Catal.* **2020**, *41*, 1772-1781.
[19] Guo, H.; Hirosaki, Y.; Qi, X.; Smith, R. L. *Renew. Energ*. **2020**, *157*, 951-958.
[20] Topolyuk, Y. A.; Nekhaev, A. I. *Mendeleev Commun.* **2018**, *28*, 93-95.
[21] Skrodczky, K.; Antunes, M. M.; Han, X.; Santangelo, S.; Scholz, G.; Valente, A. A.; Pinna, N.; Russo, P. A. *Commun. Chem.* **2019**, *2*, 129.
[22] Wu, J.; Shao, Y.; Jing, G.; Zhang, Z.; Ye, Z.; Hu, X. *J. Chem. Technol. Biotechnol.* **2019**, *94*, 3093-3101.
[23] Zhu, S.; Chen, C.; Xue, Y.; Wu, J.; Wang, J.; Fan, W. *ChemCatChem* **2014**, *6*, 3080-3083.
[24] Gao, X.; Peng, L.; Li, H.; Chen, K. *BioResources* **2015**, *10*, 6548-6564.
[25] Russo, P. A.; Antunes, M. M.; Neves, P.; Wiper, P. V.; Fazio, E.; Neri, F.; Barreca, F.; Mafra, L.; Pillinger, M.; Pinna, N.; Valente, A. A. *Green Chem*. **2014**, *16*, 4292-4305.
[26] Onkarappa, S. B.; Bhat, N. S.; Dutta, S. *Biomass Convers. Biorefin.* **2020**, *10*, 849-856.
[27] Nandiwale, K. Y.; Pande, A. M.; Bokade, V. V. Environ. Prog. Sustain. **2018**, *37*, 1736-1742.
[28] B, S. R.; P, K. K.; D, D.L.; N, L. *Catal. Today* **2018**, *309*, 269-275.
[29] Kong, X.; Zhang, X.; Han, C.; Li, C.; Yu, L.; Liu, J. *Mol. Catal.* **2017**, *443*, 186-192.
[30] Tiwari, M.S.; Gawade, A.B. ; Yadav, G.D. *Green Chem*. **2017**, *19*, 963-976.
[31] Shao, Y.; Li, Y.; Sun, K.; Zhang, Z.; Tian, H.; Gao, G.; Li, Q.; Liu, Q.; Liu, Q.; Hu, X. *Energy Technol. Ger.* **2020**, *8*, 1900951.
[32] Song, D.; An, S.; Sun, Y.; Zhang, P.; Guo, Y.; Zhou, D. *ChemCatChem* **2016**, *8*, 2037-2048.
[33] Song, D.; An, S.; Lu, B.; Guo, Y.; Leng, J. *Appl. Catal. B: Environ.* **2015**, *179*, 445-457.
[34] Song, D.; An, S.; Sun, Y.; Guo, Y. *J. Catal.* **2016**, *333*, 184-199.
[35] An, S.; Song, D.; Lu, B.; Yang, X.; Guo, Y. H. *Chem. Eur. J.* **2015**, *21*, 10786-10798.
[36] Zhang, Z.; Wang, P.; Wu, Z.; Yue, C.; Wei, X; Zheng, J.; Xiang, M.; Liu, B. *RSC Adv*. **2020**, *10*, 5690-5696.
[37] Patil, C.R.; Rode, C. V. *ChemistrySelect* **2018**, *3*, 12504-12511.
[38] Wang, Y.; Zhao, D.; Triantafyllidis, K. S.; Ouyang, W.; Luque, R.; Len, C. *Mol. Catal.* **2020**, *480*, 110630.
[39] Zhao, G.; Liu, M.; Xia, X.; Li, L.; Xu, B. *Molecules* **2019**, *24*, 1881.
[40] Zhao, D.; Prinsen, P.; Wang, Y.; Ouyang, W.; Delbecq, F.; Len, C.; Luque, R. *ACS Sustain. Chem. Eng*. **2018**, *6*, 6901-6909.
[41] Cao, Q. ; Guan, J.; Peng, G.; Hou, T.; Zhou, J.; Mu, X., *Catal. Commun.* **2015**, *58*, 76-79.
[42] Nandiwale, K.Y. ; Pande, A.M. ; Bokade, V.V. ; *RSC Adv.* **2015**, *5*, 79224-79231.

[43] Maldonado, G.M. G. ; Assary, R. S.; Dumesic, J. A.; Curtiss, L. A., *Energy Environ. Sci.* **2012**, *5*, 8990-8997.
[44] Ren, D.; Fu, J.; Li, L.; Liu, Y.; Jin, F.; Huo, Z. *RSC Adv*. **2016**, *6*, 22174-22178.
[45] Mulik, N. L.; Niphadkar, P. S. ; Bokade, V. *Res. Chem. Intermediat.* **2020**, *46*, 2309 - 2325.
[46] Chada,R. R.; Koppadi, K.S.; Enumula, S. S.; Kondeboina, M.; Kamaraju, S. R. R.; Burri, D. R. *Catal. Lett.* **2018**, *148*, 1731-1738.
[47] Wang, M.-Y. ; Su, H.; Zhai, G.-Y.; Yu, Q.-Y. ; Wang, H.-H. ; Jiang, Z.-D.; Li, X.-H.; Chen, J.-S. *Energy Technol.-Ger* **2019**, *7*, 1900271.
[48] Chaffey, D. R. ; Davies, T. E. ; Taylor, S. H. ; Graham, A. E. *ACS Sustain. Chem. Eng*. **2018**, *6*, 4996-5002.
[49] Lange, J.-P. ; Graaf, W.D. van de ; Haan, R.J. ; *ChemSusChem* **2009**, *2*, 437-441.